GA–A22990

CONF-981064--

BEHAVIOR OF ELECTRON AND ION TRANSPORT IN DISCHARGES WITH AN INTERNAL TRANSPORT BARRIER IN THE DIII–D TOKAMAK

by

C.M. GREENFIELD, C.L. RETTIG, G.M. STAEBLER, B.W. STALLARD, M.E. AUSTIN, K.H. BURRELL, J.C. DeBOO, J.S. deGRASSIE, E.J. DOYLE, P. GOHIL, R.J. GROEBNER, J. LOHR, G.R. McKEE, W.A. PEEBLES, C.C. PETTY, R.I. PINSKER, B.W. RICE, T.L. RHODES, E.J. SYNAKOWSKI, R.E. WALTZ, and L. ZHENG

DECEMBER 1998

GENERAL ATOMICS

GA–A22990

BEHAVIOR OF ELECTRON AND ION TRANSPORT IN DISCHARGES WITH AN INTERNAL TRANSPORT BARRIER IN THE DIII–D TOKAMAK

by

C.M. GREENFIELD, C.L. RETTIG,[1] G.M. STAEBLER, B.W. STALLARD,[2] M.E. AUSTIN,[3] K.H. BURRELL, J.C. DeBOO, J.S. deGRASSIE, E.J. DOYLE,[1] P. GOHIL, R.J. GROEBNER, J. LOHR, G.R. McKEE,[4] W.A. PEEBLES,[1] C.C. PETTY, R.I. PINSKER, B.W. RICE,[2] T.L. RHODES,[1] E.J. SYNAKOWSKI,[5] R.E. WALTZ, and L. ZHENG[1]

This is a preprint of a paper presented at the 17th IAEA Fusion Energy Conference, October 19–24, 1998, Yokohama, Japan, and submitted for publiction in a Special Issue of *Nuclear Fusion.*

Work supported by U.S. Department of Energy under Contracts DE-AC03-89ER51114, W-7405-ENG-48, and DE-AC02-76CH03073, and Grants DE-FG03-86ER-53266, DE-FG03-97ER54415, DE-FG03-86ER53225, and DE-FG02-92ER54139

[1]University of California, Los Angeles
[2]Lawrence Livermore National Laboratory
[3]The University of Texas at Austin
[4]University of Wisconsin, Madison
[5]Princeton Plasma Physics Laboratory

GENERAL ATOMICS PROJECT 3466
DECEMBER 1998

BEHAVIOR OF ELECTRON AND ION TRANSPORT IN DISCHARGES WITH AN INTERNAL TRANSPORT BARRIER IN THE DIII-D TOKAMAK

C.M. GREENFIELD, C.L. RETTIG,[1] G.M. STAEBLER, B.W. STALLARD,[2]
M.E. AUSTIN,[3] K.H. BURRELL, J.C. DeBOO, J.S. deGRASSIE, E.J. DOYLE,[1]
P. GOHIL, R.J. GROEBNER, J. LOHR, G.R. McKEE,[4] W.A. PEEBLES,[1]
C.C. PETTY, R.I. PINSKER, B.W. RICE,[2] T.L. RHODES,[1] E.J. SYNAKOWSKI,[5]
R.E. WALTZ, L. ZENG[1]

General Atomics
P.O. Box 5608, San Diego, California 92186-5608, U.S.A.

Abstract

We report results of experiments to further determine the underlying physics behind the formation and development of internal transport barriers (ITB) in the DIII–D tokamak. The initial ITB formation occurs when the neutral beam heating power exceeds a threshold value during the early stages of the current ramp in low-density discharges. This region of reduced transport, made accessible by suppression of long-wavelength turbulence by sheared flows, is most evident in the ion temperature and impurity rotation profiles. In some cases, reduced transport is also observed in the electron temperature and density profiles. If the power is near the threshold, the barrier remains stationary and encloses only a small fraction of the plasma volume. If, however, the power is increased, the transport barrier expands to encompass a larger fraction of the plasma volume. The dynamic behavior of the transport barrier during the growth phase exhibits rapid transport events that are associated with both broadening of the profiles and reductions in turbulence and associated transport. In some, but not all, cases, these events are correlated with the safety factor q passing through integer values. The final state following this evolution is a plasma exhibiting ion thermal transport at or below neoclassical levels. Typically, the electron thermal transport remains anomalously high. Recent experimental results are reported in which rf electron heating was applied to plasmas with an ion ITB, thereby increasing both the electron and ion transport. Although the results are partially in agreement with the usual $\vec{E} \times \vec{B}$ shear suppression hypothesis, the results still leave questions that must be addressed in future experiments.

---

[1]University of California, Los Angeles, California 90024, U.S.A.
[2]Lawrence Livermore National Laboratory, Livermore, California 94551-9900, U.S.A.
[3]The University of Texas at Austin, Austin, Texas 78712, U.S.A.
[4]University of Wisconsin, Madison, Wisconsin 53706, U.S.A.
[5]Princeton Plasma Physics Laboratory, Princeton, New Jersey 08543, U.S.A.

1. INTRODUCTION

Recent experiments on the DIII–D tokamak have been performed to further elucidate the conditions of and underlying physics behind the formation of internal transport barriers (ITB), or regions of reduced transport. Discharges with ITBs, produced by application of neutral beam preheating to low density discharges during the initial current ramp, were previously employed as the target for the highest fusion performance achieved in DIII–D [1,2]. In these plasmas, increased heating power was applied later in the discharge to expand the ITB and combine it with an H–mode edge to produce a state where neoclassical ion thermal transport was achieved throughout the entire volume.

The ITB often forms in the early phase of neutral beam heated discharges in DIII–D with negative central magnetic shear (NCS), in a region localized near the magnetic axis. The ITB region continues to develop and expand during the low-power "preheating" phase. In this paper, we will discuss the early evolution of this discharge, during the phase where the transport barrier forms and expands. The ITB expansion phase is characterized by ITB growth events superimposed on the steady evolution of the discharge. Although this behavior is consistent with theory, a puzzling feature is that in some discharges, these events correlate with low-order rational values of the safety factor q, but in others do not. This implies that there might be two different processes involved; one where the events are triggered by magnetohydrodynamic (MHD) instabilities, and another where the events are related to the behavior of microturbulence.

Another feature of the ITB discharges previously noted is that although ion thermal transport is reduced, in many cases to neoclassical levels, the behavior of the electron thermal transport often remains anomalous. Recent experiments have utilized rf electron heating to probe the underlying physics behind the electron thermal transport. The hypothesis on which these experiments were based is that electron thermal transport may be controlled by electron temperature gradient (ETG) turbulence. Although there are indications that this might be the case, other, not yet fully identified processes appear to be at work as well. Several possibilities are discusse in this paper.

2. TRANSPORT BARRIER FORMATION AND DEVELOPMENT

2.1. Initiation of the internal transport barrier

ITBs are often formed in discharges in DIII–D during the early, "preheating" phase of a discharge (Fig. 1). During this phase, low to moderate (2.5–5 MW) neutral beam power is applied to a plasma with negative central magnetic shear $\hat{s} = r/q\ \partial q/\partial r < 0$. The transport barrier forms in the core of the discharge even with this low level of power, but does not expand outward until and unless the power is increased. The requirement of sufficient power to

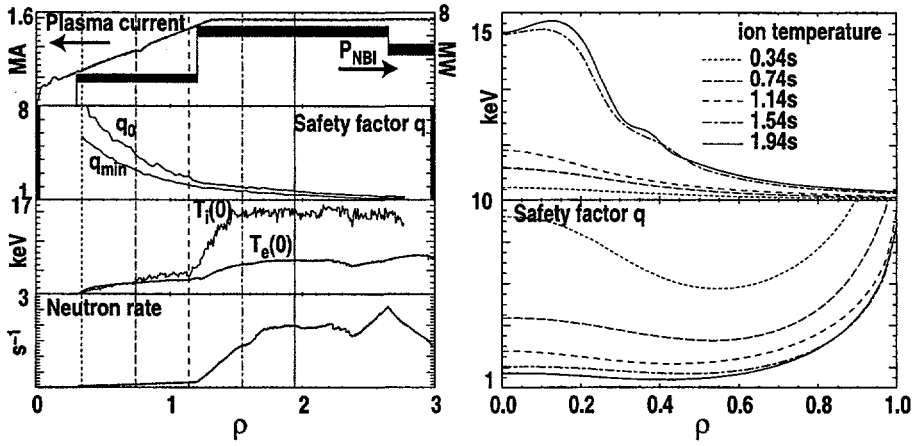

FIG. 1. Waveforms and profiles of a typical discharge with an internal transport barrier. Shot 92389, $I_P = 1.5$ MA, $B_T = -2.1$ T, $P_{NBI} = 2.5$–6.5 MW.

form the ITB implies the existence of a power threshold. In DIII–D, this threshold is approximately 2.5 MW in full-field discharges ($B_T = 2.1$ T).

These observations are in agreement with theory [3], which predicts that such transport barriers can be formed when the $\vec{E} \times \vec{B}$ shearing rate exceeds the calculated growth rates of drift wave turbulence [4]. For this stabilization mechanism to be effective, however, the drift wave turbulence must first become the leading driver of transport. Negative central magnetic shear s important here, as it, along with finite Shafranov shift of the magnetic axis, stabilize MHD instabilities which might otherwise dominate transport in this region. Also, the elevated central q values prevent the onset of sawtooth instabilities that would otherwise limit core performance.

The first consequence of the preheating is that it increases the core electron temperature and conductivity, and therefore the current diffusion time. This results in the aforementioned favorable current density profile, which is peaked off-axis. Without the early heating, the current profile would rapidly evolve to become peaked on-axis. The heating does not prevent the current profile from becoming monotonic, rather it only delays this condition. These discharges, therefore, are inherently transient. Future experiments in DIII–D will address this by applying noninductive, local current drive to maintain the current profile, either on-axis in the direction opposed to the plasma current, or off-axis in the parallel direction. This may be done using counter-injected neutral beams, electron cyclotron current drive or fast wave current drive.

The second effect, once the discharge has evolved to a state where MHD is not a leading driver of transport, is to increase the pressure and rotation gradients to generate the large $\vec{E} \times \vec{B}$ shear necessary to suppress microturbulence and therefore locally reduce transport.

2.2. Expansion of the internal transport barrier

Once the ITB is formed, the reduced transport allows the pressure and rotation gradients to further increase, thereby generating more $\vec{E}\times\vec{B}$ shear and further reduced transport. If the applied power is at or slightly above the threshold value, the barrier is formed, but remains stationary at $\rho \approx 0.3$. At higher power levels, typically 5 MW or above, the plasma enters a feedback loop where transport, $\vec{E}\times\vec{B}$ shear and fluctuations evolve toward a state of very low transport. In this condition, the ITB expands outwards to encompass a larger portion of the plasma volume (Fig. 1). The previously reported [1,2] discharges in which the ion thermal transport was reduced to neoclassical levels throughout the entire plasma were the most extreme example of this phenomenon and requires an H–mode edge. In typical discharges in DIII–D with an L–mode edge, however, the transport barrier does not expand past $\rho \approx 0.5$.

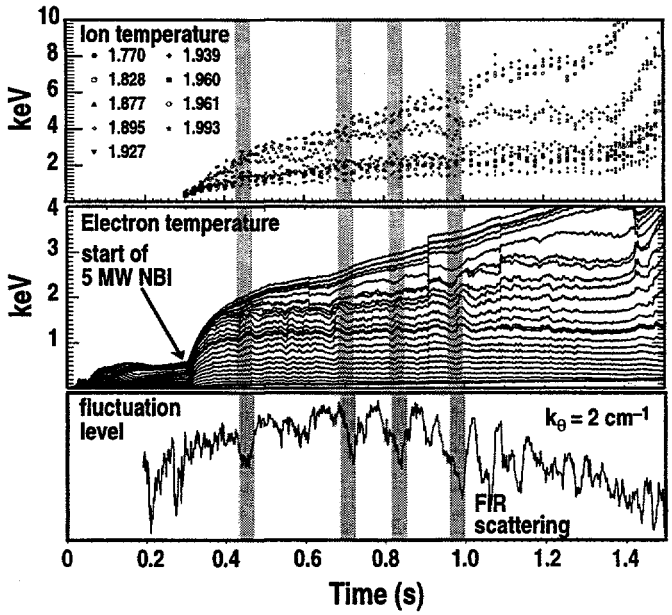

FIG. 2. Evolution of a discharge with a developing ITB during the preheating phase (0.3–1.37s). The ion and electron temperatures exhibit ITB growth events (gray bars) which correlate with transient reductions in fluctuations measured by FIR scattering. Shots 89939–89949 (composite), $I_P = 1.6$ *MA,* $B_T = -2.1$ *T,* $P_{NBI} = 5-8$ *MW.*

The barrier expansion phase of the discharge is characterized by an evolution that is anything but quiescent. During this development, stepwise growth events are observed in the otherwise steadily evolving ion temperature profile, as well as transient local decreases (Fig. 2). The steps often correlate with similar events observed in the plasma rotation and electron temperature. Also, consistent with predictions of numerical modeling of the discharge dynamics [5], transient reductions in fluctuation amplitudes are observed at the same time as the steps (Fig. 2). Measurements of the local change in electron temperature across one such event (Fig. 3) reveal the existence of a strong transport barrier, in this case at $\rho \approx 0.4$. The

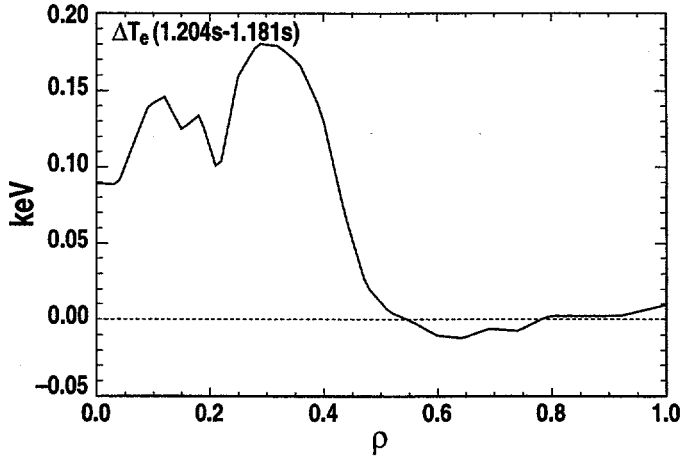

FIG. 3. The electron temperature rise during an ITB growth event is confined to inside the ITB, indicating that the ITB actually behaves as a local barrier. Shot 94100, I_P = 1.0 MA, I_P = 1.6 MA, T, P_{NBI} = 4 MW.

temperature increase is confined within the transport barrier, while the profiles outside this region are relatively unaffected.

One consideration in evaluating the data is the possibility that the "bursting" behavior is due to local or global MHD instabilities which are momentarily triggered as the safety factor q passes through low-order rational values. Although it is certainly true that the current profile is evolving during this phase, and that the minimum safety factor q_{min} does periodically pass through integer values, the transport events noted from the kinetic profiles and fluctuation measurements do not usually appear to correlate with integer q values (Fig. 4). We have reasonable confidence in this assertion for these discharges. Even a systematic error in the q profile would not bring the transport events into line with integer q crossings. Also, since the current profile is rather flat in the vicinity of the transport barrier, it is difficult to determine the exact time when integer q crossings occur. However, at least at some of the transport events, the local and minimum q values are both far enough from an integer value to make the MHD arguments implausible for this case.

There are, however, counterexamples exhibiting transport events that appear to contradict the above reasoning. In these discharges, integer q values are well correlated with the ITB growth events (Fig. 4). The reason why we observe such similar behaviors differing in their temporal correlation with integer q values in similar discharges is not well understood, and is currently under investigation. The two sets of discharge evolutions also both lead to the same state, where the ion thermal transport is reduced to neoclassical levels at and inside the ITB.

2.3. Discharges with stationary transport barriers

As indicated above, the ITB regime is inherently transient. In most cases, the entire q profile continues to monotonically decrease until it reaches unity, at which point core confinement becomes dominated by MHD instabilities and the barrier collapses. Often the ITB

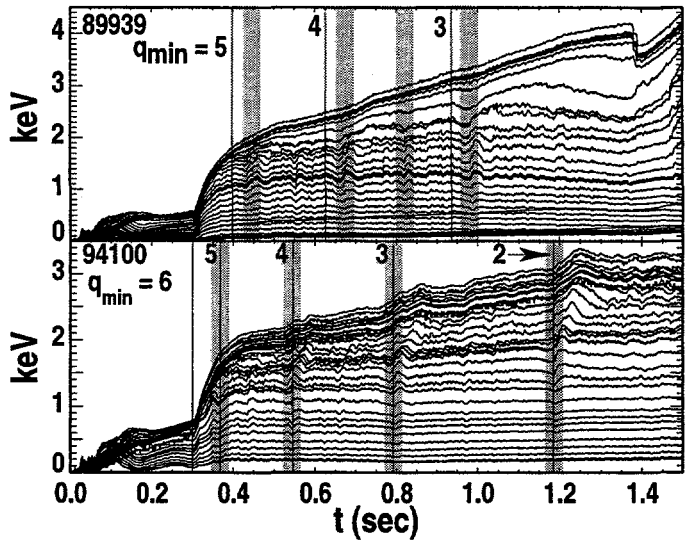

FIG. 4. The ITB growth events (gray bars) usually do not appear to correlate with integer crossings of the q profile (lines). In the first case, two events occur between $q_{min} = 4$ *and* $q_{min} = 3$*, making it unlikely that the lack of correlation is simply a systematic error in calculating the equilibrium (89939,* $I_P = 1.6$ *MA,* $B_T = -2.1$ *T,* $P_{NBI} = 5-8$ *MW.). In other cases, the barrier growth events correlate well with low-order rational values of* q_{min} *(94100,* $I_P = 1.0$ *MA,* $B_T = -2.0$ *T,* $P_{NBI} = 4$ *MW.*

is terminated even earlier by disruptions triggered by large local pressure gradients at the ITB or by an entry to H–mode (the H–mode discharges of Refs. 1 and 2 are typically at much higher heating power levels and are ELM-free). A proof of principle experiment was undertaken to verify that under the right conditions, we could in fact produce a plasma with a steady state ITB.

In these discharges, during which the plasma current (0.6 MA) and heating power (4.25 MW) were maintained at a low level, ITBs were formed which were maintained until the end of the discharge, when the heating power was reduced and the plasma current rampdown commenced (Fig. 5). Note that by the last 0.5 s of this discharge, even the electron density and current profiles had come into equilibrium.

It has been suggested that the position of the "foot" of the transport barrier might correspond to a low order rational value of the safety factor q. This appears not to be the case in most discharges in DIII–D. In this discharge, the ITB forms with the foot (defined here as the location where $\partial^2 T_i / \partial \rho^2$ is maximized) at $\rho \approx 0.4$, and remains near this location for the duration of the discharge (Fig. 5). After 2 s, a plateau, or central flat region, forms in the T_i profile. The edge of the plateau (minimum of $\partial^2 T_i / \partial \rho^2$) follows the $q = 2$ surface.

Unfortunately, this low density, low current discharge suffered from TAE-like activity [6], which caused large fast-ion losses from the core and reduced the effective confinement. The losses were also large enough that we were unable to perform a transport analysis of this discharge. When we attempted to reproduce this discharge under conditions stable to TAE-like

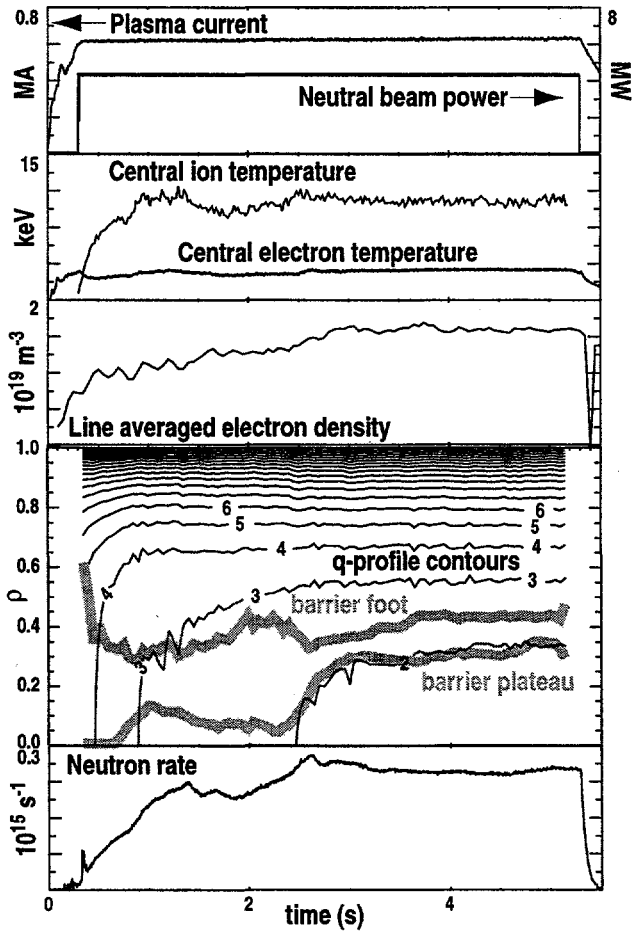

FIG. 5. A low current, low power discharge forms and maintains an ITB until the neutral beams are turned off. The temperature and density profiles are ready after 2.5 s, with the q-profile reaching a near-stationary state for the last 1.0 s. Shot 94777, $I_P = 0.6$ MA, $B_T = -1.9$ T, $P_{NBI} = 4$ MW.

modes, we were unable to sustain the transport barrier for even a short time as q_{min} rapidly dropped to and below 1, and sawtooth activity began. It is believed that this is due to neutral beam current drive (NBCD), which is made more effective when fast-ion losses are eliminated. Future experiments are planned with neutral beam counter-injection. Under these conditions, NBCD should increase, rather than decrease, q_0.

3. ANOMALOUS ELECTRON THERMAL TRANSPORT

In most plasmas, the electron diffusivity χ_e remains anomalously high even when a transport barrier is established for ions. In the discharge shown in Fig. 6, for example, the ion thermal transport has decreased to neoclassical levels throughout the plasma, but transport in the electron channel remains anomalously high. In some discharges with strongly reversed central magnetic shear, the electron diffusivity is reduced as well (Fig. 6). Whether strongly

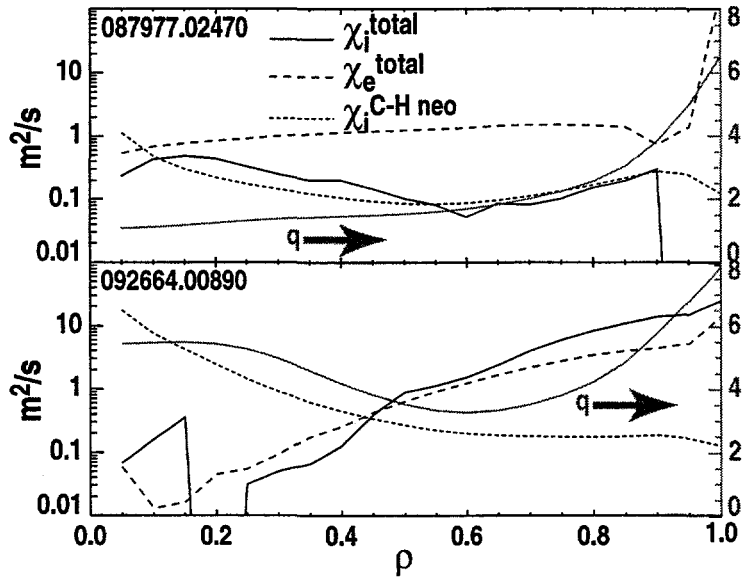

FIG. 6. Diffusivity χ and safety factor q profiles for a pair of discharges. In an ITB discharge with an ELM-free H–mode edge, the ion diffusivity is close to neoclassical everywhere in the plasma, but the electron diffusivity is considerably higher (87977, $I_P = 2.2$ MA, $B_T = -2.1$ T, $P_{NBI} = 17.55$ MW). In an L–mode discharge with an ITB and strongly reversed magnetic shear, both ion and electron thermal transport appear suppressed in the core (92664, $I_P = 1.5$ MA, $B_T = -2.1$ T, $P_{NBI} = 7.4$ MW).

reversed magnetic shear is a necessary and/or sufficient condition for electron ITB formation is not currently known.

We have identified a reproducible tool to *increase* transport in the electron channel. Applying central electron heating to a discharge with an ion transport barrier can have a large deleterious impact on transport in the electron channel. Experiments have been done in DIII–D using both electron cyclotron (ECH) and fast wave (FW) power to heat electrons in target discharges established as detailed in Section 2. The central electron temperature increases upon application of additional electron heating (Fig. 7), but far less than would be expected under conditions of constant electron diffusivities. In fact, transport analysis performed using the TRANSP [7] code indicates that the core electron diffusivity increases by a full order of magnitude on the application of this electron heating. Perhaps equally intriguing is the fact that application of 1.1 MW of (ECH) electron heating to the discharge of Fig. 7 actually results in 20%–40% reductions to the central ion temperature and impurity rotation, and associated large increases to the ion thermal and angular momentum diffusivities.

This appears not to be a direct consequence of the heating method. The results are very similar for both the FW and ECH cases, each of which exhibits increased diffusivities in the electron, ion and angular momentum channels (Fig. 8). We concentrate here on the ECH

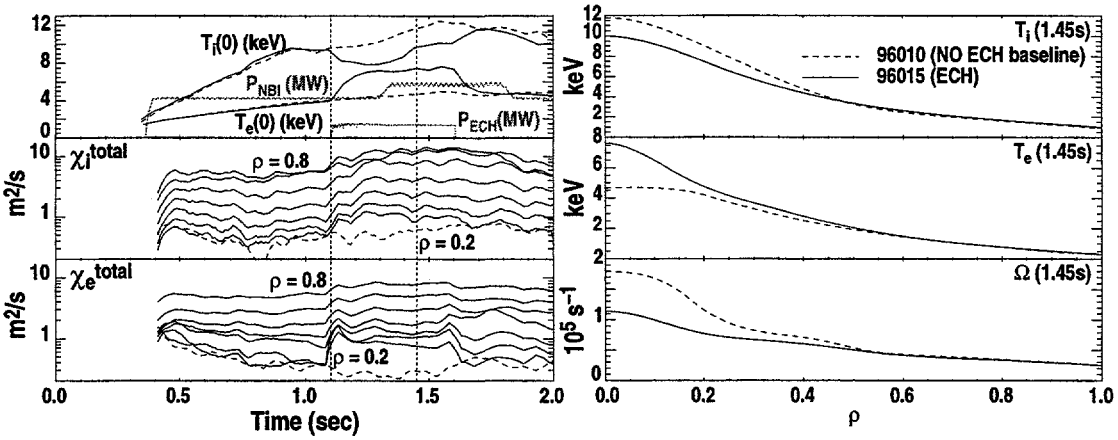

FIG. 7. Application of ECH, heating only electrons near the resonance at $\rho \approx 0$, interrupts the formation of an internal transport barrier. Core ion temperature is reduced and electron temperature increased compared to a similar discharge with no ECH (dashed lines). The inferred electron and ion diffusivities are both sharply increased during the ECH pulse. Shots 96010 (no ECH) and 96015 (1.1 MW ECH 1.1–1.6 s). $I_P = 1.6$ MA, $B_T = -2.0$ T, $P_{NBI} = 4.3–5.7$ MW.

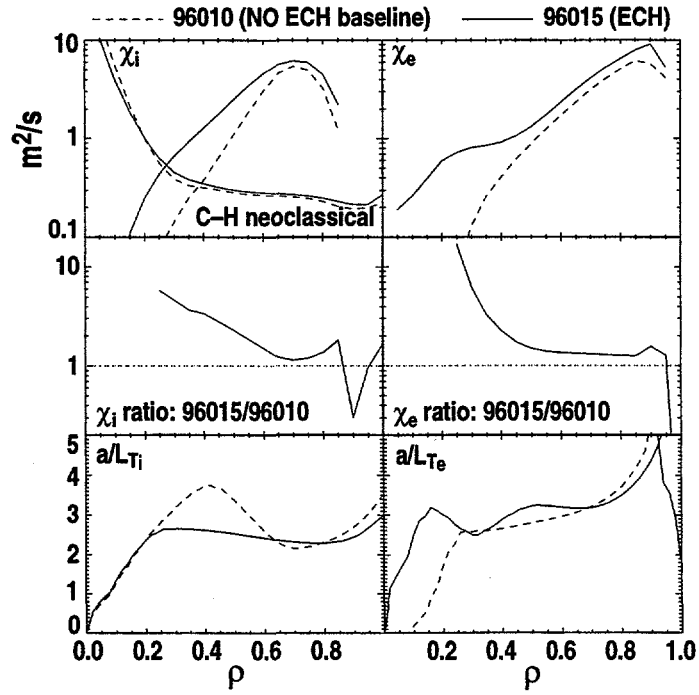

FIG. 8. Although both discharges exhibit an ion ITB, it is smaller in spatial extent in the ECH discharge. The electron diffusivity χ_e is much higher in the discharge heated by ECH. The normalized temperature gradients a / L_{Ti} and a / L_{Te} also indicate a reduced ITB with ECH. Shots 96010 (no ECH) and 96015 (1.1 MW ECH 1.1–1.6 s). $I_P = 1.6$ MA, $B_T = -2.0$ T, $P_{NBI} = 4.3–5.7$ MW.

discharge, since we have more confidence in the power deposition calculations used in the TRANSP analysis. The statements made here, however, could just as easily be made with regard to the FW heated discharges [8].

The transport behavior appears consistent with the hypothesis of $\vec{E}\times\vec{B}$ shear suppression of turbulence leading to ITB formation. The discharge heated only with neutral beams exhibits a ion ITB in this region (Fig. 8). Examination of the $\vec{E}\times\vec{B}$ shearing rate profile in this discharge (Fig. 9) indicates two maxima, with turbulence suppression most likely in the vicinities of $\rho \approx 0.2$ and $\rho \approx 0.6$. In the discharge with additional electron heating (EH), the shearing rate is sharply decreased and has collapsed to a single maxima (Fig. 9). This is reflected in the ion temperature profile as a reduction in the normalized ion temperature gradient a/L_{Ti} at $0.2 \le \rho \le 0.6$ (Fig. 8).

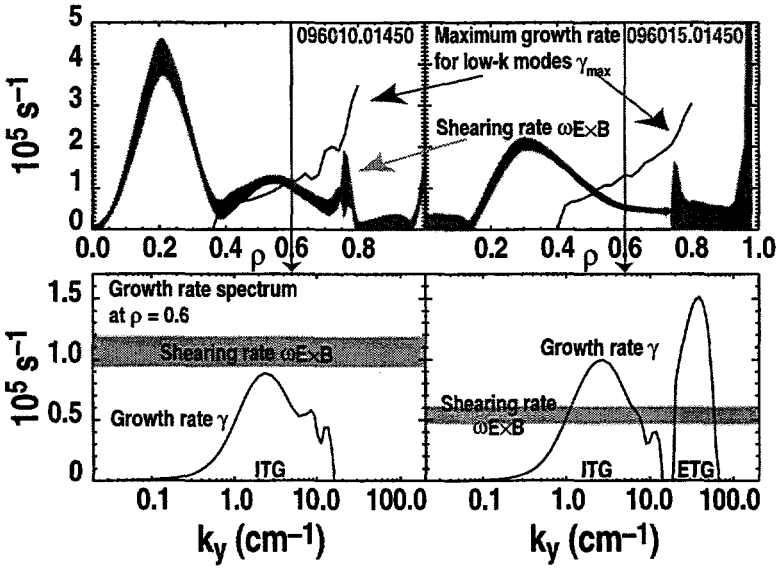

FIG. 9. GKS calculations indicate regions in both discharges where $\gamma_{max} > \omega_{E\times B}$, indicating destabilization of low-k turbulence at $\rho \ge 0.6$ (no ECH) and $\rho \ge 0.5$ (with ECH). A second region at $\rho \approx 0.4$ in the discharge without rf appears marginally stable. The reduction of the ITB in the ECH discharge results in reduced shearing rates throughout most of the plasma. At $\rho = 0.6$, the low-k growth rate in the non-rf discharge is marginal for $1 < k < 10$ cm^{-1}, and unstable in the same range of the ECH discharge due to a combination of increased growth rate and reduced shearing rate. An additional feature in the ECH discharge at high $k > 20$ cm^{-1} may indicate ETG instabilities. Shots 96010 (no ECH) and 96015 (1.1 MW ECH 1.1–1.6 s). $I_P = 1.6$ MA, $B_T = -2.0$ T, $P_{NBI} = 4.3$–5.7 MW.

Calculations of microturbulence stability have been made using a linear gyrokinetic stability (GKS) code [9] which has been extended to non-circular, finite aspect ratio equilibria [10] with fully electromagnetic dynamics [11]. The calculated maximum growth rate of long-wavelength microturbulence is shown in Fig. 9. The $\vec{E}\times\vec{B}$ shearing rate is either equaled or

exceeded at $\rho \approx 0.4$ and $\rho \approx 0.7$. Although the growth rates do not substantially increase with the application of EH, the shearing rate is reduced in the same region, indicating the loss of the ITB.

Beam emission spectroscopy (BES) measurements [12] of low-k fluctuation have been made in these discharges (Fig. 10). Consistent with the calculated shearing and growth rates, these observations indicate reduced fluctuations encompassing the transport barrier at $\rho \approx 0.5$–0.6, and no reduction in the region where the shearing rate is matched or exceeded by the growth rate. Unfortunately, BES data in the region where the barrier was eliminated with EH was not obtained, but we would expect to have seen higher levels of turbulence indicated in this region.

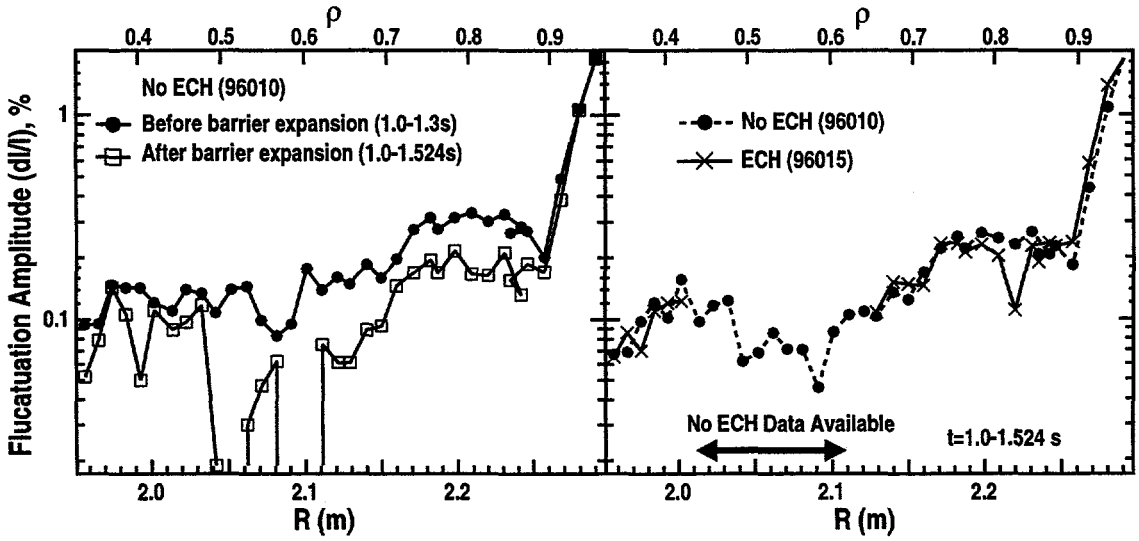

FIG. 10. In the non-rf-heated plasma, BES indicates reduced fluctuations during the increased NBI phase after 1.3 s near $\rho \approx 0.6$, with no reduction at $\rho \approx 0.4$ and a smaller reduction further out in the plasma. This appears consistent with the GKS calculations indicating regions of instability both inside and outside the transport barrier at $\rho \approx 0.6$. Data from the ECH discharge appears very similar, but data in the region where we expect the biggest difference based on the calculations was not obtained. Shots 96010 (no ECH) and 96015 (1.1 MW ECH 1.1–1.6 s). $I_P = 1.6$ MA, $B_T = -2.0$ T, $P_{NBI} = 4.3$–5.7 MW.

A slight increase in the normalized electron temperature gradient a/L_{Te} is seen in the same region with application of EH (Fig. 8). As previously stated, calculation of the growth rate spectrum at $\rho \approx 0.6$ indicates that the low-k (1–5 cm^{-1}) turbulence growth rates should be suppressed by $\vec{E} \times \vec{B}$ shear without ECH, and should become visible with ECH. An additional feature (Fig. 9) appearing in the ECH discharge at high-k (> 20 cm^{-1}) may indicate destabilization of electron temperature gradient (ETG) modes. It is believed that the ETG turbulence may be responsible for limiting a/L_{Te} in this case, but DIII–D has no diagnostics capable of observing such short-wavelength activity.

There appears to be a fundamental difference between the physics controlling transport around $\rho = 0.5$–0.6 and that at smaller radii. Dramatic reductions are seen in the both the electron and ion temperature gradients of both discharges for $\rho \leq 0.2$ (Fig. 8). Application of ECH extends the strong electron temperature gradient region inward to $\rho \approx 0.1$, and appears to have no impact on the ion temperature gradient. Throughout the region near the magnetic axis, however, no drift wave turbulence is predicted unstable for either discharge, yet the temperature gradients are clearly limited by some other physical process. One clue to the controlling process may be the appearance of high-k (12 cm^{-1}) fluctuations in far-infrared (FIR) coherent scattering measurements [13] from the discharge with ECH (Fig. 11) at $\rho \approx 0.1$. These fluctuations, at small but measurable amplitude, rotate in the electron diamagnetic direction. At the same time in similar discharges, no signal was detected at either 6 or 9 cm^{-1}.

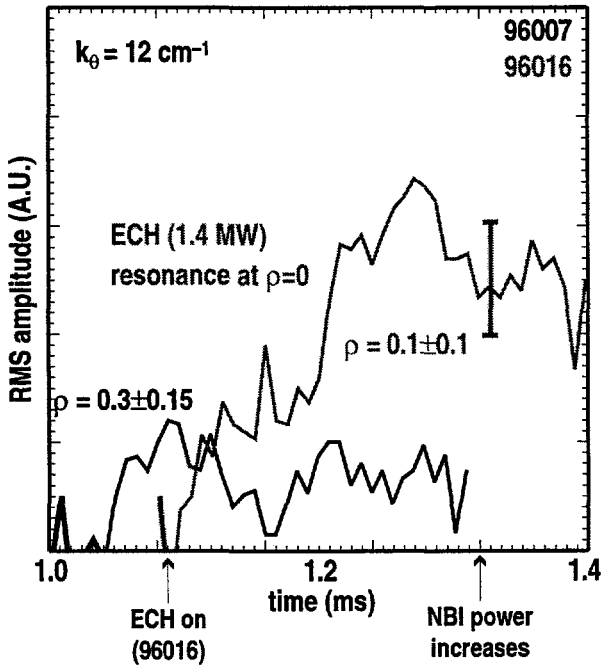

FIG. 11. FIR scattering detects a small signal at $k_\theta = 12$ cm^{-1} during the ECH pulse. The GKS calculations indicate that this is unlikely to be due to ETG activity (1.1 MW ECH 1.1–1.6 s). $I_P = 1.6$ MA, $B_T = -2.0$ T, $P_{NBI} = 4.3$–5.7 MW.

We have identified two candidates for at least some of the physics involved in this process. Both prospects are believed to preferentially impact transport in the electron channel. First, the BALOO code [14] indicates instability to the resistive interchange mode in a small region centered at $\rho \approx 0.2$ in the ECH discharge (Fig. 9). How this mode should be manifested in the plasma is not known, but it might be consistent with the high-k fluctuation measurement. A second prospect is the appearance of a collisionless microtearing mode as proposed in Ref. [15]. The potential for these modes to be present in and have an impact on these discharges is currently being evaluated. In general, they are believed capable of appearance at short wavelengths, and may be highly localized in k-space. This could be consistent with FIR scattering measurements at short wavelengths.

In these experiments, electron heating was applied during the preheating phase, prior to the increase in neutral beam power that triggers an ITB growth phase. ECH or FW electron heating appears to limit development of the ITB during the high-beam-power phase of the discharge. The resulting state is one where the temperature gradients in the vicinity of the ITB are reduced compared to the no-EH case. The reduced gradients result in reduced temperatures at smaller radii and increased diffusivities, despite the fact that locally, the normalized temperature gradients may be the same. The important physics, then, is the destabilization of low-, and perhaps high-k turbulence at the ITB location. How this occurs as a direct consequence of the central electron heating is uncertain. In addition, we see that another not yet positively identified process is at work nearer to the magnetic axis. This process may affect both the discharge with and that without additional electron heating. Investigation of this region will continue.

4. SUMMARY

Internal transport barriers are routinely produced in DIII–D by applying moderate levels of neutral beam power to low density plasmas during the current ramp. The resulting elevated central electron temperature and the associated high conductivity of the core produce a current profile that is peaked off-axis, and exhibits negative central magnetic shear. This magnetic configuration is favorable for the elimination of MHD instabilities from the core, thereby allowing the formation of an ITB.

When the ITB forms, a feedback loop involving the steep pressure and rotation gradients leads to increased $\vec{E}\times\vec{B}$ shear, which leads in turn to reduced turbulence and transport and back to the gradients again. The final state is a region of very low transport that can encompass a large portion of the plasma. The evolution leading to this state, however, is highly dynamic, exhibiting transport events that have in some, but not all, cases been associated with the saety factor profile crossing through integer values. The transport events are associated with transient reductions in turbulence and highly localized transport barrier behavior that moves outward with the "steps."

Although our understanding of thermal transport in the ion channel has improved considerably, we have not yet come to the same level of understanding of the electron channel. In experiments where we probed the transport response to electron heating, both the ion and electron channels were impacted. This is partially due to a failure of the ITB to completely develop during the high power phase of the discharge. Both long- and short-wavelength turbulence are predicted to have been destabilized in the region where the ITB would have continued to develop in the ECH discharge. Without more complete measurements of fluctuations in the plasma, we cannot be certain that such turbulence actually appears in the experiment. The impact on the temperature profiles, however, appears consistent with the modeling. Other processes impacting transport closer to the magnetic axis have not yet been positively identified. Both experimental and modeling efforts to understand these effects will continue in the future.

ACKNOWLEDGMENTS

The authors gratefully acknowledge the contributions of the DIII–D Operations and RF groups without whose efforts the experiments could not have been carried out. Also, M. Kotschenreuther of the University of Texas and W. Dorland of the University of Maryland contributed valuable insight in their discussions with one of the authors (G.M.S.).

This is a report of work supported by U.S. Department of Energy Contracts DE-AC03-89ER51114, W-7405-ENG-48, and DE- AC02-76CH03073, and Grants DE-FG03-86ER-53266, DE-FG03-97ER54415, DE-FG03-86ER-53225, and DE-FG02-92ER54139.

REFERENCES

[1] SCHISSEL D.P., et al., Proc. 16th IAEA Fusion Energy Conf. Montreal, 1996 (IAEA, Vienna, 1997) Vol. 1, p. 463.
[2] GREENFIELD, C.M., et al., Phys. Plasmas **4** (1997) 1596.
[3] WALTZ, R.E., et al., Phys. Plasmas **1** (1994) 2229.
[4] BURRELL, K.H., Phys. Plasmas **4** (1997) 1499 .
[5] NEWMAN, D.E., et al., Phys. Plasmas **5** (1998) 938.
[6] HEIDBRINK, W.W., ''What is the 'Beta-Induced Alfvén Eigenmode' '', submitted to Phys. Plasmas (1998).
[7] HAWRYLUK, R.J., in Proc. of the Course in Physics Close to Thermonuclear Conditions, Varenna, 1979 (Commission of the European Communities, Brussels, 1980).
[8] STAEBLER, G.L., et al., ''Electron Thermal Transport in Enhanced Core Confinement Regimes'', to be published in Proc. 25th EPS Conf., Prague (1998).
[9] KOTSCHENREUTHER, M., Bull. Am. Phys. Soc. **37** (1992) 1432.
[10] MILLER, R.L., et al., Phys. Plasmas **5** (1998) 973.
[11] WALTZ, R.E., DORLAND, W., private communication (1998).
[12] McKEE, G.R., et al., ''The Beam Emission Spectroscopy Diagnostic on the DIII–D Tokamak'', to be published in Rev. Sci. Instrum. (1999).
[13] PHILIPONA, T., et al., Rev. Sci. Instrum. **61** (1990) 3007.
[14] MILLER, R.L., et al., private communication (1998).
[15] KOTSCHENREUTHER, M., et al., these Proceedings.